

# Testing of Hybrid Quantum-Classical K-Means for Nonlinear Noise Mitigation

Ark Modi\*, Alonso Viladomat Jasso<sup>†</sup>, Roberto Ferrara\*, Christian Deppe\*, Janis Nötzel<sup>†</sup>,  
Fred Fung<sup>‡</sup>, Maximilian Schädler<sup>‡</sup>

\* Institute for Communications Engineering (LNT),

<sup>†</sup> Emmy Noether Group for Theoretical Quantum Systems Design  
Technical University of Munich, D-80333 Munich, Germany

<sup>‡</sup> Optical and Quantum Laboratory, Munich Research Center

Huawei Technologies Düsseldorf GmbH, Riesstr. 25-C3,80992 Munich, Germany

Email: {ark.modi, viladomat.jasso, roberto.ferrara, christian.deppe, janis.noetzel}@tum.de

{fred.fung, maximilian.schaedler}@huawei.com

**Abstract**—Nearest-neighbour clustering is a powerful set of heuristic algorithms that find natural application in the decoding of signals transmitted using the  $M$ -Quadrature Amplitude Modulation ( $M$ -QAM) protocol. Lloyd et al. proposed a quantum version of the algorithm that promised an exponential speed-up. We analyse the performance of this algorithm by simulating the use of a hybrid quantum-classical implementation of it upon 16-QAM and experimental 64-QAM data. We then benchmark the implementation against the classical  $k$ -means clustering algorithm. The choice of quantum encoding of the classical data plays a significant role in the performance, as it would for the hybrid quantum-classical implementation of any quantum machine learning algorithm. In this work, we use the popular angle embedding method for data embedding and the swap test for overlap estimation. The algorithm is emulated in software using Qiskit and tested on simulated and real-world experimental data. The discrepancy in accuracy from the perspective of the induced metric of the angle embedding method is discussed, and a thorough analysis regarding the angle embedding method in the context of distance estimation is provided. We detail an experimental optic fibre setup as well, from which we collect 64-QAM data. This is the dataset upon which the algorithms are benchmarked. Finally, some promising current and future directions for further research are discussed.

**Index Terms**—Quantum  $k$  nearest-neighbour, Quantum Machine Learning, Quantum Computing,  $k$ -Means Clustering, 6G Communication, Quadrature Amplitude Modulation, Quantum-Classical Hybrid Algorithms

## I. INTRODUCTION

Quantum information processing is a method that started out to revolutionize the current theory of computation. Much has been done in showing its theoretical potential, with several candidate algorithms offering quadratic, exponential or even greater speed-ups. One question is whether part of this potential can be exploited with NISQ devices, which is often been impeded by hurdles during implementation. Hybrid-quantum classical systems are a popular option for the implementation of quantum algorithms due to the lack of stable quantum memory (QRAM) and due to the realisation that only certain tasks are suitable to be offloaded for quantum processing. Here, we compare the classical and hybrid quantum-classical

implementation of a machine learning algorithm applied to the decoding problem of classical optical-fiber communication.

Quantum-enhanced Machine Learning, using quantum algorithms to learn quantum or classical systems, has sometimes promised even exponential speed-ups over classical machine learning. Due to the significance of classical machine learning today, there is a lot of focus on such quantum machine learning algorithms for tomorrow's world. A number of works such as [1]–[6] have showcased theoretical algorithms and experimental implementations that naturally give confidence that other quantum algorithms, including quantum machine learning ones, might eventually lead to industrial quantum algorithms with a speed up. Many of these methods claim to offer exponential speedups over the analogous classical algorithms. However there exist significant gaps between the-oretical prediction and implementation.

We demonstrate the problems and possible opportunities when applying the quantum  $k$  nearest-neighbour clustering algorithm to the problem of decoding  $M$ -QAM signals. It is known that the  $k$ -means clustering algorithm can be used for phase estimation in optical fibers [7], [8]. Though the quantum version of this algorithm [6] promises an exponential speed-up, its usefulness in NISQ devices and end-to-end classical systems is under debate [5], [9]. Due to such difficulties, we study the advantages and drawbacks as seen from a the  $M$ -QAM application.

In Section II, we review the problem of signal processing through optic fibre cables and detail the experimental setup. In Section III, we describe the encoding method and the quantum circuit used for simulation. After this, the results of the simulation of hybrid quantum-classical  $k$ -means are described in Section IV. We end with some promising current and future directions for further research [9]–[16].

## II. PROBLEM AND DATA DESCRIPTION

In QAM multiple bits are conveyed in each time interval and carrier symbol by dividing the phase space of the carrier wave of fixed frequency, and designating each space to a unique bitstring. Signals are prepared to lie in the phase space

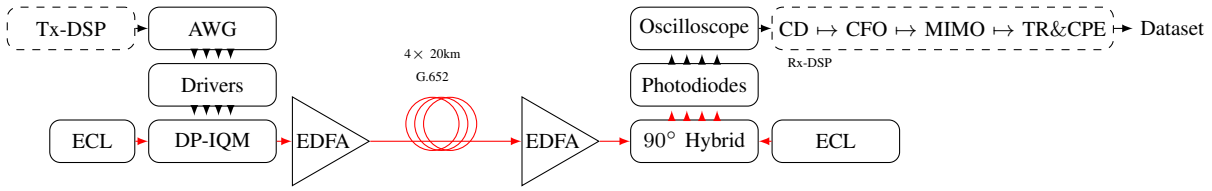


Fig. 1. Experimental setup over a 80 km G.652 fiber link at optimal launch power of 6.6 dBm.

corresponding to the required bitstring by modulating the amplitude of two carrier waves separated by  $90^\circ$  (for example, sine and cosine waves of the same frequency) and superposing them. The receiver coherently separates the waves by using the orthogonality of the two waves. QAM can achieve arbitrarily high spectral efficiencies by setting a suitable constellation size, limited only by the noise level and linearity of the channel [17].

### A. Experimental Setup for Data Collection

The dataset consists of a launch power sweep of 80 km optic fibre transmission of coherent 80 GBd dual polarization (DP)-64QAM with a gross data rate of 960Gb/s. 15% overhead for FEC and 3.47% overhead for pilots and training sequences have been used, leading to a net bit rate of 800Gb/s. The experimental setup to capture this real-world database is shown in Fig. 1. A more detailed explanation of the data and setup can be found in [16]. The received raw signals have preprocessed by the receiver to create the dataset upon which clustering could be performed as a final decoding step. The signals were also normalized to fit the initial transmission values (alphabet). The data consists of 4 sets with different launch powers, corresponding to different noise levels during transmission: 2.7dBm, 6.6dBm, 8.6dBm, and 10.7dBm. The average launch power in Watts (W) can be calculated as follows:

$$P_{(W)} = 1W \cdot 10^{P_{(dBm)}/10}/1000 = 10^{(P_{(dBm)}-30)/10}W.$$

Figure 2 shows the received data (all 5 instances of transmission) for the dataset with the least noise (2.7dBm), and Fig. 3 shows the received data (all 5 instances of transmission) for the dataset with most noise (10.7dBm).

For the generation of the 16-QAM data, the received signal is modelled as (amplitude damping is ignored):

$$\hat{s} := e^{i(\varphi_b + \Phi)} \cdot s + \mathbf{N}. \quad (1)$$

Here  $s$  is the transmitted signal,  $\Phi$  is a random phase acquired during transmission which is distributed according to a normal distribution with zero mean and variance  $\sigma_\Phi$  [18],  $\mathbf{N}$  is additive zero mean Gaussian noise of variance  $\sigma_N$  (AWGN) [19], and  $\varphi_b$  is an unknown induced by birefringence that is assumed to be constant over some period of time.

## III. METHODOLOGY

### A. Data Embedding Procedure

Classical data needs to be converted into quantum states for processing in a quantum computer due to the poor coherence

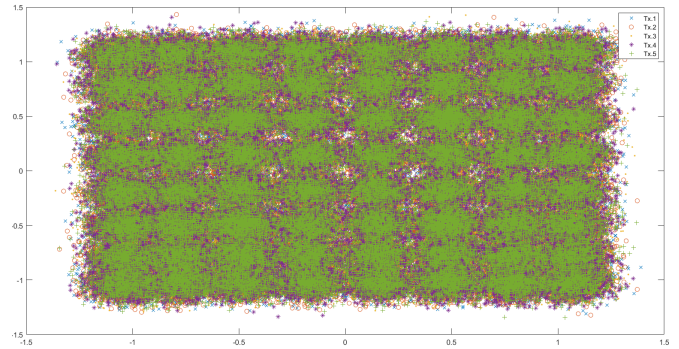


Fig. 2. The data detected by the receiver from the least noisy (2.7dBm noise) channel. All 5 iterations of transmission are depicted together.

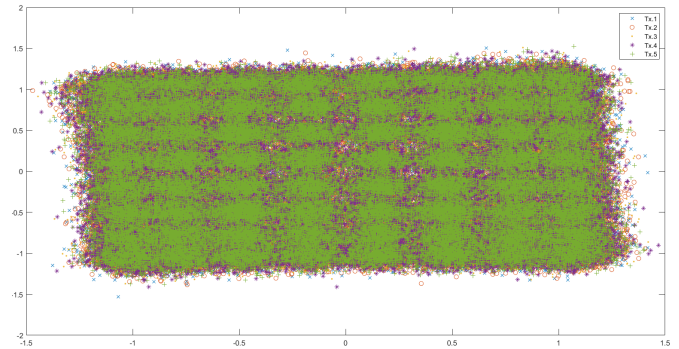


Fig. 3. The data detected by the receiver from the noisiest (10.7dBm noise) channel. All 5 iterations of transmission are depicted together.

times and very limited number of qubits in current NISQ (Noisy Intermediate Scale Quantum) devices. One of the most popular methods of data encoding is angle embedding since it needs only  $\mathcal{O}(1)$  operations regardless of how many data values need to be encoded. Distance estimation between two data points  $(x_1, y_1)$  and  $(x_2, y_2)$  using angle embedding consists of preparing quantum states through a unitary operation with the data point encoded in it. The two dimensional data vectors are normalised and transformed as [15]

$$x'_i = \frac{\pi}{2} \left( \frac{x_i}{\sqrt{x_i^2 + y_i^2}} + 1 \right) \quad y'_i = \frac{\pi}{2} \left( \frac{y_i}{\sqrt{x_i^2 + y_i^2}} + 1 \right). \quad (2)$$

This mapping enables us to encode the data points as

$$|\psi\rangle = U(x'_1, y'_1) |0\rangle \quad \text{and} \quad |\phi\rangle = U(x'_2, y'_2) |0\rangle, \quad (3)$$

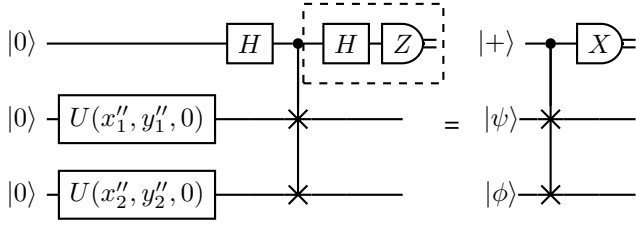


Fig. 4. Quantum circuit of the swap Test

where  $U$  is the unitary

$$U(\theta, \gamma) := \begin{pmatrix} \cos \frac{\theta}{2} & -\sin \frac{\theta}{2} \\ e^{i\gamma} \sin \frac{\theta}{2} & e^{i\gamma} \cos \frac{\theta}{2} \end{pmatrix}. \quad (4)$$

However, one can see that this form of embedding is not injective. If two points in the plane lie on the same radial line, Eq. (2) will yield identical values of  $x'_i$  and  $y'_i$ . This is not ideal for k-means clustering since it is quite possible to have several points with the same phase. To counter this problem, one can calculate and store the amplitude of each vector, and then use that to estimate the distance.

Instead, we preprocess the data to achieve an injective data embedding scheme. We do so by using the following a different transformation for the 2-dimensional data vector:

$$x''_i = \frac{\pi}{2} (\bar{x}_i + 1) \quad y''_i = \frac{\pi}{2} (\bar{y}_i + 1), \quad (5)$$

where  $\{\bar{x}, \bar{y}\}_i = \frac{\{x, y\}_i}{r_{\max}}$  and  $r_{\max} := \max_i \{\sqrt{x_i^2 + y_i^2}\}$ . The two transformed vectors are then still encoded in the same way (angle embedding) as

$$|\psi\rangle = U(x''_1, y''_1) |0\rangle \quad |\phi\rangle = U(x''_2, y''_2) |0\rangle. \quad (6)$$

A distinct advantage of an injective embedding is that the output of the quantum circuit is eligible to be used directly for classifying the point, avoiding further post-processing steps. In [16], we use the inverse stereographic projection to calculate the parameters of the embedding.

### B. Quantum circuit for overlap estimation

Once the states have been prepared by encoding the classical data, they are processed through the quantum circuit shown in Fig. 4 to yield information about the overlap between the states. This circuit corresponds to the swap test. The swap test is a method commonly used in quantum computing for learning overlap estimation between two quantum states, first developed in [20]. The task of finding the overlap is accomplished by measuring the output of the ancilla qubit of the swap test circuit many times. The number of times this is repeated is known as the number of shots. Since we only measure the ancilla, the other two qubits are theoretically available for future reuse; in other words, the swap test performs a non-destructive measurement. We point out that this is wasteful in a hybrid quantum-classical system since quantum states are not stored or reused. A better option, as mentioned in [16], is the Bell State measurement test,

which performs a destructive measurement - saving not only a quantum gate but also a qubit.

### C. Swap Test Probabilities and Distance Loss Function

In this section, we prove that the output of Fig. 4 can be used for distance estimation, and calculate the end-to-end result of our procedure. Given two input states  $|\psi\rangle$  and  $|\phi\rangle$ , independent of the form of embedding, the swap test yields a Bernoulli random variable  $M$  with values in  $\{0, 1\}$  defined via:

$$\mathbb{P}(M = m) = \frac{1}{2}(1 + (-1)^m |\langle \psi | \phi \rangle|^2) \quad (7)$$

and variance

$$\text{Var}(M) = \mathbb{P}(M = 0) \cdot \mathbb{P}(M = 1) = \frac{1 - |\langle \psi | \phi \rangle|^4}{4}.$$

We use the unbiased estimator:

$$\mathbb{P}(M = 1) \approx \frac{1}{n} \sum_{j=1}^n m_j, \quad (8)$$

where  $m_1, \dots, m_n \in \{0, 1\}$  are the measurement results obtained from the repeated measurement of the ancilla qubit of the swap test circuit.

After assuming the form of embedding described in Section III-A, one can calculate the expression for the projection between the two qubits as follows:

$$\langle \phi | \psi \rangle = \cos\left(\frac{\pi}{4}(\bar{x}_1 + 1)\right) \cos\left(\frac{\pi}{4}(\bar{x}_2 + 1)\right) + e^{i\frac{\pi}{2}(\bar{y}_1 - \bar{y}_2)} \sin\left(\frac{\pi}{4}(\bar{x}_1 + 1)\right) \sin\left(\frac{\pi}{4}(\bar{x}_2 + 1)\right). \quad (9)$$

Using this, we get our final distance estimate or ‘distance loss function’:

$$\mathbb{P}(1) = \frac{1}{4} \left( 1 - \cos\left(\frac{\pi}{2}\bar{x}\right) \cos\left(\frac{\pi}{2}\bar{y}\right) \right) \quad (10)$$

One can see through Eq. (10) that the hybrid quantum-classical implementation of this algorithm provides a different loss function for the distance between  $(x_1, y_1)$  and  $(x_2, y_2)$  than the Euclidean distance. The overlap  $\langle \phi | \psi \rangle$  is estimated from the probabilities of the swap test and the expression of the estimator (Eqs. (7) and (8)). As we can see from Eq. (10), the swap test using both standard angle embedding and our form of it does not enable calculation of the true Euclidean distance. It uses, in fact, a completely different distance estimate. It is illustrative to pick the point  $(0, 0)$  (origin) and see how the distance loss function with other points  $(x, y)$  varies - see Figs. 5 and 6. One can see that with our method of rescaling, the loss function is smoother at origin. The advantage of our method can be brought into sharper focus with another example - distance estimation between  $(x, 0)$  and  $(y, 0)$  i.e., between 2 points on the x-axis. Traditional angle embedding yields the loss function depicted in Fig. 7 while our version yields Fig. 8.

The performance of the swap test can also be increased by using more elaborate testing strategies [10]. Performance bounds are made visible in [10, Fig. 2]. However, from the NISQ perspective, the joint measurements over many copies

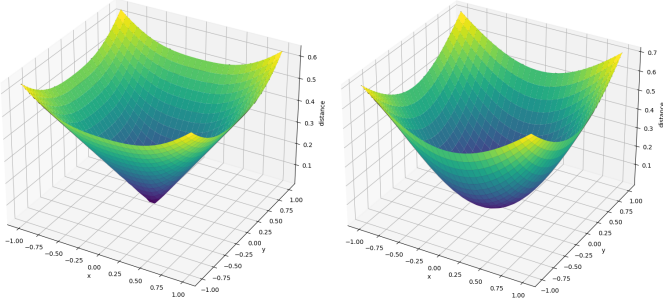


Fig. 5. Standard angle embedding distance loss function between  $(x, y)$  and  $(0, 0)$

Fig. 6. Our version of the Angle embedding loss function between  $(x, y)$  and  $(0, 0)$  with  $r_{max} = 1$

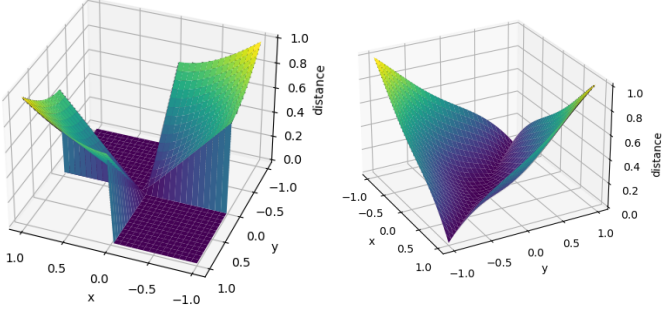


Fig. 7. Standard angle embedding distance loss function for 2 points on the x-axis

Fig. 8. Our version of the Angle embedding loss function for 2 points on the x-axis with  $r_{max} = 1$

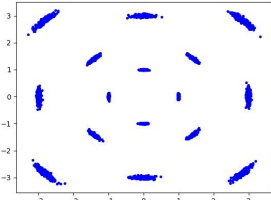


Fig. 9. Parameters are  $\sigma_\Phi = 0.05$ ,  $\sigma_N = 0.01$ ,  $\varphi_b = 0$ .

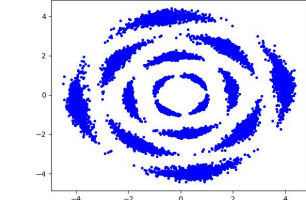


Fig. 10. Parameters are  $\sigma_\Phi = 0.2$ ,  $\sigma_N = 0.04$ ,  $\varphi_b = \frac{3\pi}{10}$ .

of the quantum states representing the data points contradicts the idea of a simplified system design and limiting the number of qubits and gates.

## IV. PERFORMANCE AND RESULTS

### A. Characterisation using 16-QAM data

The accuracy of the quantum  $k$ -means code is first reviewed through experiments performed on *generated 16-QAM noisy data*. Figures 9 and 10 are representative of the kind of 16-QAM datasets upon which the algorithms were performed.

The first test shows how the number of shots used for the swap-test affects accuracy (see Fig. 11). Next, we demonstrate the effect of the fixed phase noise of the data on the accuracy (see Fig. 12). Lastly, an accuracy heat-map by varying the noise levels is produced (shown in Fig. 13). The confusion matrix of the experiment is shown in Fig. 14.

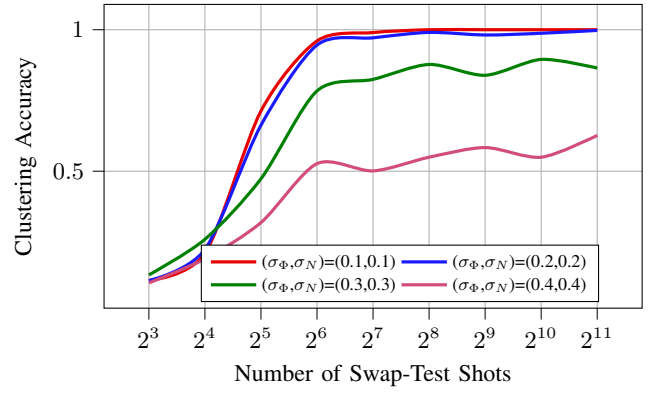


Fig. 11. Number of shots vs. Accuracy

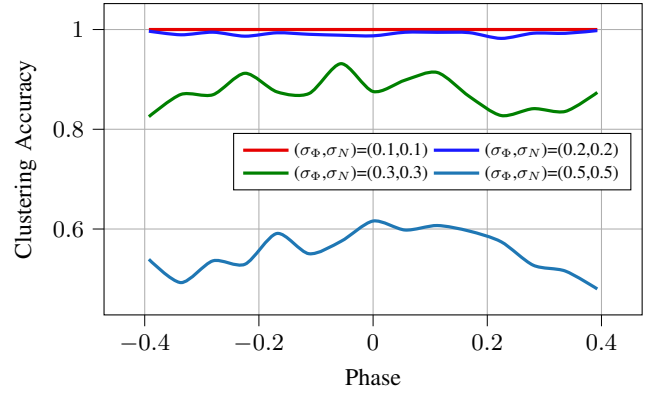


Fig. 12. Mean Phase Noise vs. Accuracy

### B. Testing using optical fibre real data

As mentioned before, the experimentally collected real-world data is 64-QAM data transmitted via optic fibre, and there are 4 sets of data with different noise levels during transmission: 2.7dBm, 6.6dBm, 8.6dBm, and 10.7dBm. Tables I to IV summarize the accuracy, number of points and maximum number of allowed algorithm iterations for datasets with channel noises of 2.7, 6.6, 8.6 and 10.7dBm respectively. The number of shots for overlap estimation using the quantum circuit was kept constant at 50 shots.

As seen in Tables I to IV, the hybrid quantum-classical implementation of quantum  $k$ -means clustering using angle embedding performs noticeably worse than classical  $k$ -means in terms of accuracy. This accuracy discrepancy stems from *the process of data embedding*. The use of angle embedding caused the distance estimated using the loss function from Eq. (10) to become more susceptible to noise in the optic fibre cable. This is further discussed in the next section.

The time taken for execution of the hybrid quantum-classical and classical  $k$ -means clustering algorithms on the real data differ greatly due to the high computational time of simulating quantum devices in a classical computer. This implementation can be applied into programming a real quantum chip, which could improve the time performance. However, currently quantum gate delays are  $\sim 1000\times$  classical gate

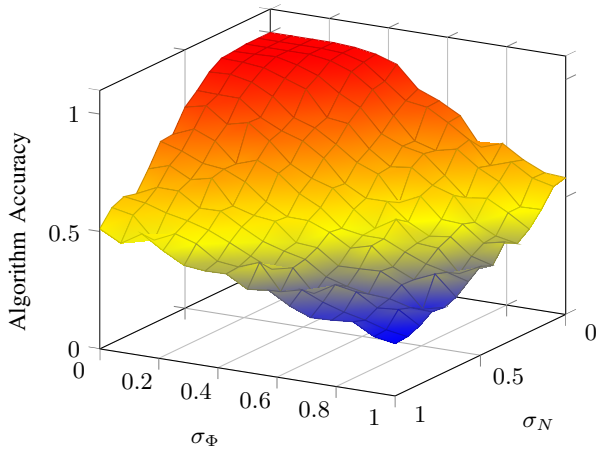


Fig. 13. Heat-map plot of the accuracy with varying noise parameters.

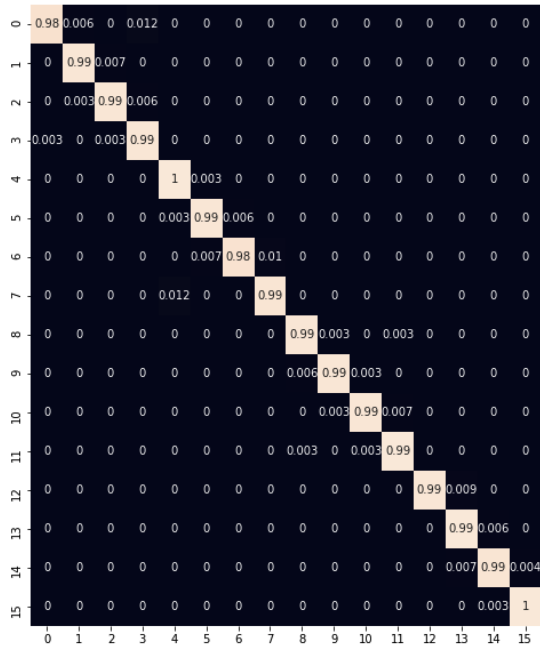


Fig. 14. The accuracy of performing the quantum clustering algorithm with angle embedding in simulation using 5 distance estimates per circuit.

delays. An estimation of the processing time it would take to cluster a 16-QAM dataset with 5000 2D data points using angle encoding follows. Gate times for the 7-qubit IBMQ Casablanca are in the range of 305 - 760 ns, the average gate time being 443 ns. Using the IBM Quantum Platform, which uses the available basis gates for implementation, we obtain that for angle embedding the circuit depth is 22. Hence we estimate the time taken for one shot of the swap test to be from 6710 to 16720 ns, and 9746 ns on average. To compute 1 iteration with 16 centroids, 5000 datapoints and 50 shots per distance estimation, the number of swap test shots needed is  $16 \cdot 5000 \cdot 50 = 4 \cdot 10^6$ . Ignoring the pre-processing steps, the QPU time will therefore be 26.84 to 66.88 seconds, 38.984 seconds on average - much slower than current classical com-

Total No. of Points		Accuracy (%)		Max. iterations	
Quantum	Classical	Quantum	Classical	Quantum	Classical
320	320	79.5	88.5	5	5
640	640	83.4	88.5	5	5
1280	1280	83.5	87.3	5	5

TABLE I  
EXPERIMENTS FOR 2.7 dBm

Total No. of Points		Accuracy (%)		Max. iterations	
Quantum	Classical	Quantum	Classical	Quantum	Classical
320	320	78.0	85.2	5	5
640	640	82.0	87.7	5	5
1280	1280	82.4	87.7	5	5

TABLE II  
EXPERIMENTS FOR 6.6 dBm

Total No. of Points		Accuracy (%)		Max. iterations	
Quantum	Classical	Quantum	Classical	Quantum	Classical
320	320	79.1	87.4	5	5
640	640	80.9	87.1	5	5
1280	1280	83.2	87.6	5	5

TABLE III  
EXPERIMENTS FOR 8.6 dBm

Total No. of Points		Accuracy (%)		Max. iterations	
Quantum	Classical	Quantum	Classical	Quantum	Classical
320	320	72.6	80.2	5	5
640	640	74.1	82.5	5	5
1280	1280	77.7	82.3	5	5

TABLE IV  
EXPERIMENTS FOR 10.7 dBm

puters. As the quantum hardware technology node advances and gate times reduce (faster circuits, more stable qubits, less quantum error correction), the quantum algorithm will become more competitive time-wise.

## V. DISCUSSION AND CONCLUSION

The core idea for the paper was to analyse the strengths and weaknesses of the quantum  $k$ -means clustering proposed by Lloyd et al. in the NISQ context to cluster QAM data. The proposed algorithm in [6] assumes a quantum random access memory for state preparation, which allows them to access the data in quantum parallel. Since at this time there are no commercially available practical realisations of such a quantum RAM, we decided to use a hybrid quantum-classical approach, where only the distance estimation part of the algorithm is done using a quantum computer. The rest of the algorithm is executed on a classical computer. Naturally, this required us to embed classical data into quantum states - this introduces the classical data loading problem, leading us to question if there really is any quantum advantage. For the preparation of quantum states, we decided to use angle embedding since it has a simple  $\mathcal{O}(1)$  implementation using current basis gates. Using the unitary as defined in Eq. (4) leads effectively to a  $M$ -way classification using a cosine kernel [21], [22]. This makes the expectation of quantum advantage seem more suspect since a cosine kernel can be easily computed classically. We also show that when using the defined unitary (a product of rotation gates with a global phase), one does not produce the Euclidean distance but (as one would expect from a cosine

kernel) a trigonometric ‘loss function’. We predict the loss function, and we see that this ‘distance loss function’ is less steep than a paraboloid - this led us to believe that the performance would be adversely affected. This prediction is indeed supported by the simulation. To stress the point further: *we predict and show that the hybrid quantum-classical k-means algorithm has an inferior performance to classical k-means simply due to the process of angle embedding.* This is a theoretically predicted loss in performance; even when the simulations are performed without quantum noise, the algorithm’s performance is expected to be deficient. With the addition of quantum noise, one would expect the accuracy of the hybrid quantum-classical algorithm to suffer even further. However, in spite of this worse loss function, we see that the accuracy is surprisingly high. Despite a completely different distance estimate, our accuracy was on par in the case of 16-QAM and slightly worse for 64-QAM. It seems that as the non-linear noise and the number of clusters increases, the performance of the angle embedding loss function decreases.

Our approach opens the door for other distance loss functions which could yield even better accuracy than the classical algorithm. This approach is similar to that of constructing ‘Quantum Kernels’ for SVM and other kernel based learning methods [23], [24]. We can construct ‘quantum distance loss functions’ which can then be used for clustering of data. These functions can also be used in applications such as spectral clustering or nearest mean classification. Such other kinds of data embedding, where the unavoidable step of data embedding can in fact be used to one’s advantage, is explored in [16] in particular, it discusses the very promising stereographic embedding.

Another important direction of future work is to benchmark the performance of the algorithms on standard clustering datasets. An investigation to be carried out is to find use-cases better tailored to the hybrid implementation.

#### ACKNOWLEDGEMENT

This work was funded by the TUM-Huawei Joint Lab on Algorithms for Short Transmission Reach Optics (ASTRO). This project has received funding from the DFG Emmy-Noether program under grant number NO 1129/2-1 (JN) and by the Federal Ministry of Education and Research of Germany in the programme of ‘‘Souveran. Digital. Vernetzt.’’. Joint project 6G-life, project identification number: 16KISK002, and of the Munich Center for Quantum Science and Technology (MC-QST). We would also like to acknowledge fruitful discussions with Stephen DiAdamo and Fahreddin Akalin during the initial stages of the project.

#### REFERENCES

[1] F. Arute, K. Arya, R. Babbush *et al.*, ‘‘Quantum supremacy using a programmable superconducting processor,’’ *Nature*, vol. 574, p. 505–510, 2019. [Online]. Available: <https://www.nature.com/articles/s41586-019-1666-5>

[2] M. Schuld and F. Petruccione, *Supervised Learning with Quantum Computers*, ser. Quantum Science and Technology. Springer International Publishing, 2018. [Online]. Available: <https://books.google.de/books?id=1zpsDwAAQBAJ>

[3] F. P. M. Schuld, I. Sinayskiy, ‘‘An introduction to quantum machine learning,’’ *arXiv:1409.3097 [quant-ph]*, 2014.

[4] I. Kerenidis and A. Prakash, ‘‘Quantum Recommendation Systems,’’ in *8th Innovations in Theoretical Computer Science Conference (ITCS 2017)*, ser. Leibniz International Proceedings in Informatics (LIPIcs), C. H. Papadimitriou, Ed., vol. 67. Dagstuhl, Germany: Schloss Dagstuhl–Leibniz-Zentrum fuer Informatik, 2017, pp. 49:1–49:21. [Online]. Available: <http://drops.dagstuhl.de/opus/volltexte/2017/8154>

[5] I. Kerenidis, J. Landman, A. Luongo, and A. Prakash, ‘‘q-means: A quantum algorithm for unsupervised machine learning,’’ *arXiv:1812.03584*, 2018.

[6] S. Lloyd, M. Mohseni, and P. Rebentrost, ‘‘Quantum algorithms for supervised and unsupervised machine learning,’’ *arXiv:1307.0411*, 2013.

[7] L. Pakala and B. Schmauss, ‘‘Non-linear mitigation using carrier phase estimation and k-means clustering,’’ in *Photonic Networks; 16. ITG Symposium*. VDE, 2015, pp. 1–5.

[8] J. Zhang, W. Chen, M. Gao, and G. Shen, ‘‘K-means-clustering-based fiber nonlinearity equalization techniques for 64-qam coherent optical communication system,’’ *Optics express*, vol. 25, no. 22, pp. 27 570–27 580, 2017.

[9] E. Tang, ‘‘Quantum principal component analysis only achieves an exponential speedup because of its state preparation assumptions,’’ *Physical Review Letters*, vol. 127, no. 6, Aug 2021. [Online]. Available: <http://dx.doi.org/10.1103/PhysRevLett.127.060503>

[10] M. Fanizza, M. Rosati, M. Skotiniotis, J. Calsamiglia, and V. Giovannetti, ‘‘Beyond the swap test: Optimal estimation of quantum state overlap,’’ *Physical Review Letters*, vol. 124, no. 6, Feb 2020. [Online]. Available: <http://dx.doi.org/10.1103/PhysRevLett.124.060503>

[11] A. Harrow, ‘‘Applications of coherent classical communication and the schur transform to quantum information theory,’’ Ph.D. dissertation, Massachusetts Institute of Technology, Massachusetts Institute of Technology, Cambridge, MA, 2005, 2005.

[12] A. W. H. Dave Bacon, Isaac L. Chuang, ‘‘Efficient quantum circuits for schur and clebsch-gordan transforms,’’ *arXiv:quant-ph/0407082*, 2004.

[13] D. Bacon, I. L. Chuang, and A. W. Harrow, ‘‘The quantum schur and clebsch-gordan transforms: I. efficient qudit circuits,’’ in *Proceedings of the Eighteenth Annual ACM-SIAM Symposium on Discrete Algorithms*, ser. SODA ’07. USA: Society for Industrial and Applied Mathematics, 2007, p. 1235–1244.

[14] H. Krovi, ‘‘An efficient high dimensional quantum schur transform,’’ *arXiv:1804.00055v2*, 2019.

[15] S. DiAdamo, C. O’Meara, G. Cortiana, and J. Bernab e-Moreno, ‘‘Practical quantum k-means clustering: Performance analysis and applications in energy grid classification,’’ 2021. [Online]. Available: <https://arxiv.org/abs/2112.08506>

[16] A. Viladomat Jasso, A. Modi, R. Ferrara, C. Deppe, J. N otzel, F. Fung, and M. Sch adler, ‘‘Quantum and quantum-inspired stereographic k nearest-neighbour clustering,’’ *Entropy*, vol. 25, no. 9, 2023. [Online]. Available: <https://www.mdpi.com/1099-4300/25/9/1361>

[17] B. Microsystems, ‘‘Digital modulation efficiencies.’’ [Online]. Available: [https://web.archive.org/web/20110430132506/http://www.barnardmicrosystems.com/L4E\\_comms\\_2.htm](https://web.archive.org/web/20110430132506/http://www.barnardmicrosystems.com/L4E_comms_2.htm)

[18] L. Kunz, M. G. A. Paris, and K. Banaszek, ‘‘Noisy propagation of coherent states in a lossy Kerr medium,’’ *J. Opt. Soc. Am. B*, vol. 35, no. 2, pp. 214–222, Feb 2018. [Online]. Available: <http://josab.osa.org/abstract.cfm?URI=josab-35-2-214>

[19] H. Ghozlan and G. Kramer, ‘‘Interference focusing for mitigating cross-phase modulation in a simplified optical fiber model,’’ in *2010 IEEE International Symposium on Information Theory*, 2010, pp. 2033–2037.

[20] J. W. Harry Buhman, Richard Cleve and R. de Wolf, ‘‘Quantum fingerprinting,’’ *arXiv:quant-ph/0102001*, 2001.

[21] C. Blank, D. K. Park, J.-K. K. Rhee, and F. Petruccione, ‘‘Quantum classifier with tailored quantum kernel,’’ *npj Quantum Information*, vol. 6, no. 1, p. 41, 2020.

[22] M. Schuld, ‘‘Supervised quantum machine learning models are kernel methods,’’ 2021.

[23] V. Havlic ek, A. D. C orcoles, K. Temme, A. W. Harrow, A. Kandala, J. M. Chow, and J. M. Gambetta, ‘‘Supervised learning with quantum-enhanced feature spaces,’’ *Nature*, vol. 567, no. 7747, pp. 209–212, mar 2019. [Online]. Available: <https://doi.org/10.1038%2F541586-019-0980-2>

[24] Y. Liu, S. Arunachalam, and K. Temme, ‘‘A rigorous and robust quantum speed-up in supervised machine learning,’’ *Nature Physics*, vol. 17, no. 9, pp. 1013–1017, 2021.